

Characterization of Titanium Oxide Films Prepared by the Template-Stripping Method

Fernanda F. Rossetti, Ilya Reviakine,[†] and Marcus Textor*

Laboratory for Surface Science and Technology, Department of Materials, Swiss Federal Institute of Technology (ETH), Zürich, Switzerland

Received February 18, 2003. In Final Form: July 16, 2003

Titanium is a widely used biomaterial, and there is, therefore, considerable interest in studying the processes occurring at its surface. A suitable in situ investigation technique is atomic force microscopy (AFM), which, however, requires very flat substrates. In the case of gold, the so-called "template-stripping method" has allowed the successful preparation of surfaces that are atomically flat over large areas. The method is based on the evaporation of gold onto atomically flat surfaces of freshly cleaved mica, which is subsequently stripped off. Cacciafesta et al. (*Langmuir* **2000**, *16*, 8167–8175) have applied this method for preparing model titanium (oxide) surfaces for AFM investigation. The focus of the present study was the characterization of the chemical and topographical characteristics of the resulting surface. In particular, it was found that mica could not be completely removed from the titanium during the stripping step unless a thin layer of carbon was present between the titanium and the mica. In this study, a layer of amorphous carbon was artificially introduced between the two materials, but it is possible that the carbon naturally present in the micas can play a similar role. Detailed investigation by spectroscopic (angle-resolved X-ray photoelectron spectroscopy, depth profiling, X-ray photoelectron diffraction) and imaging methods (AFM) lead to the conclusion that—on samples without a carbon interface—the mica layer is at most a few unit cells thick and is nearly confluent.

Introduction

Protein adsorption is one of the first steps in the cascade of events that follow the exposure of a material to biological milieu.¹ Examples of such instances are plentiful, but most relevant to the current work are cases of sensing devices exposed to biological fluids, catheters, and prosthetic devices—such as orthopaedic implants and vascular grafts—introduced into a body. The functionality of both biosensors and implants is directly related to the properties of their surfaces with respect to nonspecific protein adsorption.²

Designing model surfaces with controlled, well-defined surface properties is one approach to defining the basic principles that govern protein–surface³ (and therefore material–body) interactions. A complementary approach is to investigate the properties of materials, especially those which perform well when implanted (such as titanium), with respect to protein adsorption.^{4–6} In this case, it is most crucial to have the surface's physicochemical properties characterized by a variety of complementary methods, for otherwise drawing general conclusions from such studies becomes hardly possible. This necessitates the use of a combination of classical, UHV surface-analytical methods—such as X-ray photoelectron spec-

troscopy (XPS)⁷—and techniques capable of following protein adsorption in situ, in near-native conditions, such as atomic force microscopy (AFM)⁸ (see, for instance, Kim et al.⁹).

Investigation of protein-adsorption behavior on the titanium oxide surface is of significance to the biomedical industry due to the widespread use of titanium in dental and orthopaedic implants, heart valves, and vascular stents.¹⁰ Titanium devices implanted into the body are covered with a layer of oxide, and it is this oxide layer that is responsible for the favorable biocompatibility properties of titanium implants.¹¹

A novel method of preparing titanium oxide samples was recently introduced by Cacciafesta et al.¹² It is based on the so-called template-stripping method originally designed for the preparation of ultraflat gold surfaces by Hegner and Wagner¹³—summarized in Figure 1. Essentially, it consists of evaporating the metal onto the surface of mica (a layered mineral which presents clean, atomically flat terraces when cleaved) at high temperature, gluing the free metal surface onto a solid support (glass or silica), and finally removing the mica in a so-called

(7) Briggs, D.; Seah, M. P. *Practical Surface Analysis*, 2nd ed.; John Wiley & Sons: Chichester, U.K., 1990; Vol. 1.

(8) Binnig, G.; Quate, C. F.; Gerber, C. *Phys. Rev. Lett.* **1986**, *56*, 930–933.

(9) Kim, D. T.; Blanch, H. W.; Radke, C. J. *Langmuir* **2002**, *18*, 5841–5850.

(10) *Titanium in Medicine: Material Science, Surface Science, Engineering, Biological Responses and Medical Applications*; Brunette, D. M., Tengvall, P., Textor, M., Thomsen, P., Eds.; Springer-Verlag: Heidelberg and Berlin, 2001.

(11) Textor, M.; Sittig, C. E.; Frauchiger, V.; Tosatti, S.; Brunette, D. M. Properties and Biological Significance of Natural Oxide Films on Titanium and Its Alloys. In *Titanium in Medicine: Material Science, Surface Science, Engineering, Biological Responses and Medical Applications*; Thomsen, P., Ed.; Springer-Verlag: Heidelberg and Berlin, 2001; pp 171–230.

(12) Cacciafesta, P.; Humphris, A. D. L.; Jandt, K. D.; Miles, M. J. *Langmuir* **2000**, *16*, 8167–8175.

(13) Hegner, M.; Wagner, P.; Semenza, G. *Surf. Sci.* **1993**, *291*, 39–46.

* To whom correspondence should be addressed at ETH Zürich, Oberflächentechnik, Wagistrasse 2, CH-8952 Schlieren, Switzerland. E-mail: marcus.textor@mat.ethz.ch.

[†] Current address: Department of Chemical Engineering, University of Houston, Houston, TX.

(1) Kasemo, B. *Surf. Sci.* **2002**, *500*, 656–677.

(2) Wisniewski, N.; Reichert, M. *Colloids Surf., B* **2000**, *18*, 197–219.

(3) Ostuni, E.; Chapman, R. G.; Liang, M. N.; Meluleni, G.; Pier, G.; Ingber, D. E.; Whitesides, G. M. *Langmuir* **2001**, *17*, 6336–6343.

(4) Burkett, S. L.; Read, M. J. *Langmuir* **2001**, *17*, 5059–5065.

(5) Cacciafesta, P.; Hallam, K. R.; Watkinson, A. C.; Allen, G. C.; Miles, M. J.; Jandt, K. D. *Surf. Sci.* **2001**, *491*, 405–420.

(6) Höök, F.; Vörös, J.; Rodahl, M.; Kurrat, R.; Boni, P.; Ramsden, J. J.; Textor, M.; Spencer, N. D.; Tengvall, P.; Gold, J.; Kasemo, B. *Colloids Surf., B* **2002**, *24*, 155–170.

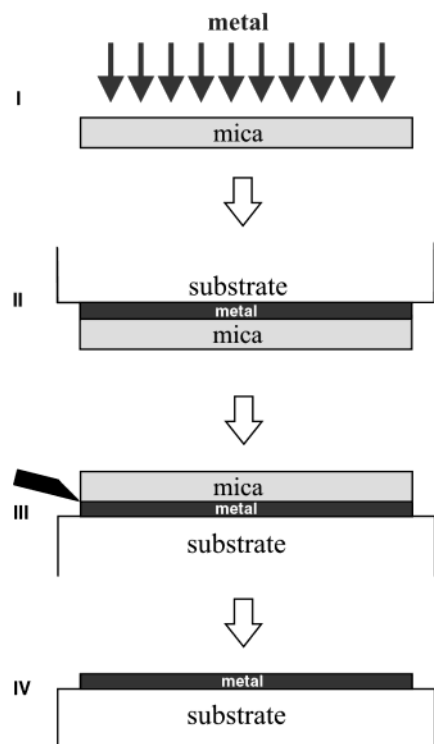


Figure 1. Principle of the template-stripping method. (I) The metal is evaporated onto a heated surface of freshly cleaved mica in an ultrahigh vacuum. Some of the samples used in this study were prepared by evaporating the metal onto a mica sheet precoated with a thin layer of carbon rather than onto the clean mica surface. (II) The metal side of the metal-coated mica is glued to a glass slide or a silicon wafer substrate with epoxy glue. Note that the metal–mica sandwich ($\sim 1.2 \times 1.2 \text{ cm}^2$) is larger than the silicon wafer ($\sim 1 \times 1 \text{ cm}^2$). (III) The mica is stripped off to leave, ideally, a clean, flat, metal surface (shown in IV). If carbon-coated mica is used in step I, the surface of the metal remains covered with the carbon after mica is cleaved, and only after a plasma-cleaning step does the metal oxide surface become exposed.

“stripping” step, Figure 1. This preparation method allows the titanium oxide surface to be studied by both types of techniques mentioned above (i.e., XPS and, especially, AFM), while the direct analysis by AFM of clinically used sample surfaces, as well as those prepared by sputtering, is made difficult by surface roughness limitations.^{12,14}

Gold, however, is a noble metal, while titanium is characterized by rather high reactivity and has a propensity for forming solid solutions (and eventually compounds) with, for example, oxygen and carbon.¹⁵ It was therefore of interest to investigate the structure of the titanium (oxide)–mica interface, and to study in detail the physicochemical characteristics of the surface exposed after mica is stripped away (Figure 1), since detailed knowledge of the properties of the latter are required for studying the protein adsorption on it.

Materials and Methods

Preparation of Titanium Films. The titanium samples used in this study originated from two sources. A number of samples were kindly given to us by P. Cacciafesta and K. Jandt (University of Bristol, U.K.). These are referred to as the “Bristol samples”.

(14) Tosatti, S.; Michel, R.; Textor, M.; Spencer, N. D. *Langmuir* **2002**, *18*, 3537–3548.

(15) Textor, M.; Freese, H. L.; Volas, M. G.; Wood, J. R. Titanium and Its Alloys in Biomedical Engineering. In *Encyclopedia of Materials: Science and Technology*; Mahajan, S., Ed.; Elsevier: Oxford, 2001; Vol. 10, pp 9374–9381.

The rest of the samples were prepared in-house, following either an identical procedure¹² based on the template-stripping method originally developed for the preparation of ultraflat gold surfaces by Hegner and co-workers¹³ or a modified version described below.

The standard procedure began with the in situ radiative heating of freshly cleaved muscovite mica (Unaxis, Balzers, Liechtenstein) for a period of 20 h at 300 °C. A 200 nm thick layer of titanium (99.9% purity, Unaxis) was subsequently thermally evaporated onto the mica at a rate of 0.1 nm/s for the first 20 nm and 0.17 nm/s for the remaining 180 nm. Annealing for 12 h at 300 °C followed the evaporation step, before the samples were cooled to room temperature at 10 °C/min. All steps took place in a BAE 370 vacuum coating system (Bal-Tec, Balzers, Liechtenstein) at pressures below 1×10^{-3} Pa. The thickness of the evaporated layers was monitored with an integrated quartz crystal deposition controller (Inficon XTC/2, Leybold, Switzerland).

The modified protocol entailed coating of freshly cleaved mica with a thin layer of amorphous carbon in a BAE 120 vacuum coating system (Bal-Tec) at a pressure below 1×10^{-2} Pa. The thickness of the carbon layer was varied by changing the coating time and determined by AFM (see below) to be between 6 and 20 nm for various samples. A stream of nitrogen was used to blow off coarse pieces of carbon and dust before using the carbon-coated mica as a substrate in the titanium evaporation procedure described above.

Titanium–mica sandwiches (1.2 by 1.2 cm^2) were subsequently glued, metal face down, onto silicon wafers of $1 \times 1 \text{ cm}^2$ area with a liquid two-component epoxy glue (Epo-tek 377, Polyscience, Cham, Switzerland). Leaving the 2 mm rim on each side of the silicon wafer prevented the glue from contaminating the top surface of the sample before and after stripping. The amount of glue was just enough to wet the surface. Its low viscosity ensured conformal contact between the glue and both surfaces. The glue was cured at 150 °C for 60 min. Mica was stripped off immediately before use with an adhesive tape. The electrical conductivity of the surface was used as an indication of the exposure of metallic titanium at the surface after the stripping process.

Plasma Treatment. Oxygen plasma, generated with a PDC-32 G plasma cleaner/sterilizer (Harrick, Ossining, NY) connected to a Pfeiffer Duo 2.5A rotary vacuum pump (Balzers, Liechtenstein), was used for oxidizing the titanium surfaces and for removing the carbon from the stripped samples that had a carbon layer at the mica–titanium interface. The exposure time of the samples to plasma was varied between 2 and 10 min. The power of the instrument was set to “high” for all experiments.

X-ray Photoelectron Spectroscopy and X-ray Photoelectron Diffraction. Routine XPS spectra were recorded on a SAGE 100 (SPECS, Berlin, Germany) using a nonmonochromatic Mg K α radiation source operating at 240 W (12 kV, 20 mA) and at a takeoff angle of the photoelectrons of 90°. The electron detector voltage was 2100 V, and the pass energy was 50 and 14 eV for survey and detailed spectra, respectively. The work function of the spectrometer was 4.3 eV. The pressure of the chamber remained below 9×10^{-6} Pa throughout the analysis.

Depth profiling by XPS was performed on a PHI 5700 from the Physical Electronics Division, Perkin-Elmer Corp. (Eden Prairie, MN) equipped with an argon sputtering device, using a non-monochromatic Al K α radiation source operating at 350 W (14 kV, 25 mA). The work function was 4.2 eV, and the pressure of the measuring chamber was kept below 5×10^{-8} Pa.

Angle-resolved XPS and X-ray photoelectron diffraction (XPD) measurements were performed at the University of Fribourg (Switzerland) in the Solid State Physics Group of Prof. L. Schlappbach, on a ESCA1-EAC-2000 from Omicron (Taanusstein, Germany), in both cases using a Mg K α radiation source operating at 240 W (12 kV, 20 mA) and at takeoff angles of 15°, 40°, 65°, and 90° (for angle-resolved XPS).

For evaluation purposes, all spectra were referenced to the aliphatic hydrocarbon C 1s signal at 285.0 eV. Data were fitted following a Shirley iterative background subtraction.¹⁶ Photoionization cross-sections determined by Scofield¹⁷ were used in the quantitative analysis.

(16) Shirley, D. A. *Phys. Rev. B* **1972**, *5*, 4709.

(17) Scofield, J. H. *J. Electron Spectrosc. Relat. Phenom.* **1976**, *8*, 129–137.

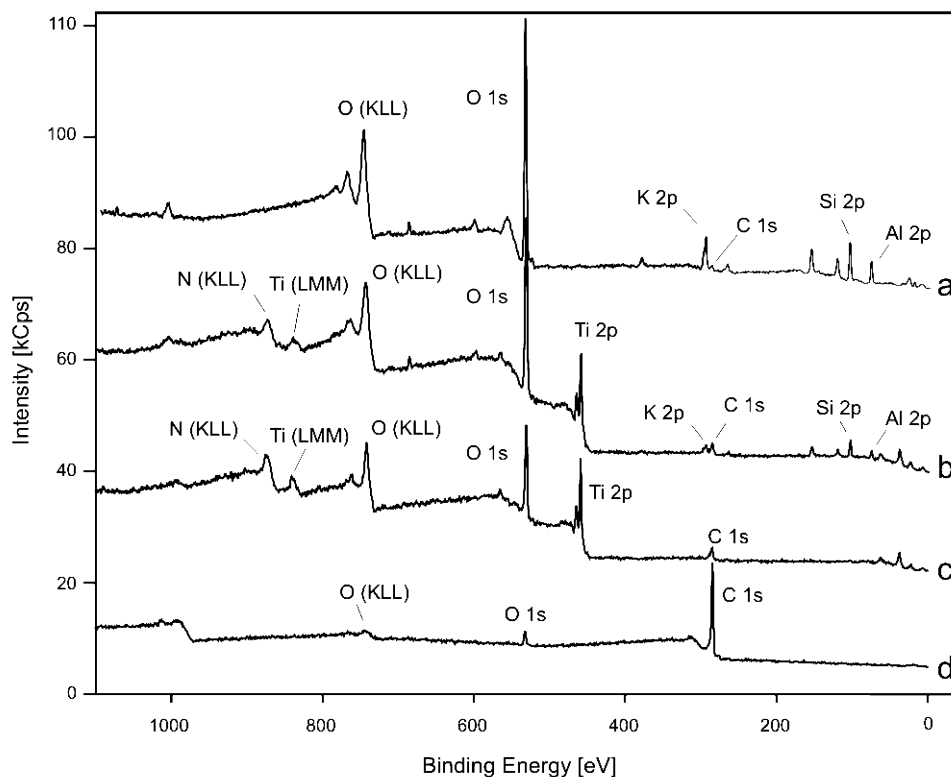


Figure 2. Elemental composition of the surfaces of the Ti samples prepared by the template-stripping method. Survey XPS spectra of mica (a) and of three different titanium samples after the mica is stripped (b–d, recorded under identical conditions) are shown. Curve b shows a spectrum of a sample prepared following the conventional template-stripping method,¹² while a spectrum recorded on a carbon-coated sample after it has been treated with oxygen plasma is shown in (c). For comparison, a spectrum recorded on a carbon-coated sample before oxygen plasma treatment is shown in (d). In addition to the peaks arising from titanium and oxygen, peaks arising from mica (i.e., Al 2p, K 2p, and Si 2p) are clearly visible in the titanium sample prepared by the conventional template-stripping method (b). They are, however, absent from the sample prepared with the carbon-coating step (c, d), indicating that its surface is completely free of mica.

Atomic Force Microscopy. AFM measurements were performed in contact mode with a Nanoscope IIIa (Digital Instruments (DI), San Diego, CA) with oxide-sharpened Si₃N₄ tips mounted on triangular cantilevers with spring constants of 0.58 N/m (specified by the manufacturer). Images of the titanium surfaces and of mica were acquired in deionized water using a fluid cell from DI. The determination of the carbon layer thickness on carbon-coated mica samples was carried out in air. Images were flattened and plane-fitted as required.

Results

The titanium–mica interface was characterized by a number of different methods based on XPS. Routine analysis of the surface-elemental composition was followed by depth profiling and angle-resolved XPS—to investigate the distribution of the elements present as a function of depth—and by X-ray photoelectron diffraction¹⁸—to ascertain if any of the elements, specifically titanium, were ordered in the plane of the interface. AFM was used to obtain complementary topographic information about the surface.

Some of the samples used in the analysis were a gift from P. Cacciafesta and K. Jandt and are referred to as “Bristol samples”. The rest of the samples were prepared in-house, following either the conventional template-stripping protocol described by Cacciafesta¹² or a modification thereof, in which an intermediate carbon layer was introduced between titanium and mica (Figure 1). These are referred to as “Zürich samples” and “carbon-coated samples”, respectively.

Elemental Composition of the Surfaces Prepared by the Template-Stripping Method. The question of foremost importance is whether the surfaces obtained after the mica–titanium sandwiches are cleaved (Figure 1) are, indeed, mica-free. To ascertain that, and to determine the chemical nature of the titanium species present at the surface, the samples were subjected to routine XPS analysis immediately following the removal of the mica by mechanical stripping. It was found that elements typical of mica (K, Al, and Si; Figure 2) were always present on samples prepared by the conventional template-stripping method. This applies to both fresh samples (the Zürich samples) and those stored for a period of time (the Bristol samples, Table 1).

For comparison purposes, mica—from the same batch as that used in the preparation of the Bristol samples—was also analyzed by XPS (Figure 2a). The ratio of the atomic percentage of Si to that of Al in that mica sample was found to be 1.21 ± 0.01 . A similar value of 1.11 ± 0.16 was obtained on the titanium surfaces after the mica was stripped (Table 1), supporting the conclusion that it was, indeed, mica that was detected on the surface after stripping (as opposed, for example, to contamination from the glue). A slightly different value for the Si-to-Al ratio— ~ 1.04 —can be found in the literature.¹⁹ The slight discrepancy can be due to variations in the composition of micas from different sources, differences in the XPS setup (e.g., angle of emission), or differences in the quantification scheme (e.g., sensitivity factor base).

(18) Osterwalder, J. *Arabian J. Sci. Eng.* **1990**, *15*, 274–291.

(19) O’Donoghue, M. *American nature guides—rocks and minerals*; Gallery Books: New York, 1990.

Table 1. Elemental Composition of the Template-Stripped Titanium Surfaces Determined by XPS^a

	Ti (%) 7.9, 2p	O (%) 2.85, 1s	C (%) 1.0, 1s	Si (%) 0.865, 2p	Al (%) 0.574, 2p	K (%) 4.04, 2p
B-2 (a)	13.9	59.9	7.1	11.2	7.4	0.6
	6.8	48.0	20.8	12.6	9.8	1.9
	14.7	58.2	8.6	9.0	8.8	0.6
B-2 (b)	10.4	55.7	16.1	10.0	6.7	1.2
B-3	5.1	53.8	6.5	16.5	12.3	5.3
	2.1	54.7	2.8	18.8	15.0	6.0
	2.3	54.2	3.5	18.4	15.1	5.9
B-4	12.6	55.9	12.1	9.4	8.0	1.9
	13.3	56.9	16.2	7.4	4.8	1.3
B-5	9.3	56.8	8.8	11.8	10.5	2.8
	7.1	54.6	6.1	15.8	12.5	3.9
B-6	<i>9.0</i>	<i>51.6</i>	<i>11.0</i>	<i>13.8</i>	<i>11.0</i>	<i>3.5</i>
	<i>9.8</i>	<i>49.4</i>	<i>15.1</i>	<i>12.0</i>	<i>10.5</i>	<i>3.2</i>
	<i>3.5</i>	<i>55.1</i>	<i>11.6</i>	<i>18.5</i>	<i>8.6</i>	<i>2.3</i>
B-7	<i>10.6</i>	<i>56.3</i>	<i>14.9</i>	<i>7.5</i>	<i>8.0</i>	<i>2.7</i>
Z-6	13.3	59.8	4.1	12.7	8.8	1.3
Z-7	17.9	59.9	3.9	6.4	9.3	2.6
Z-8	14.2	46.8	5.8	13.2	15.2	4.9
Z-9	14.0	49.7	6.7	12.9	13.7	3.1

^a Samples prepared in Bristol and in Zürich are labeled with indices "B" and "Z", respectively. The Scofield factors used in the calculations (left) and the orbital names (right) are indicated under the element symbols in the column heads. All measurements, except those indicated in italics, refer to plasma-cleaned samples. Multiple rows for one sample indicate that measurements were performed at various locations on the sample. Sample B-2 (a) was measured after additional stripping (B-2 (b)), but no improvement with respect to the removal of the mica could be detected.

Additional mechanical stripping of surfaces that had mica residue on them did not lead to an improvement (Table 1; cf. sample B-2 before (a) and after (b) additional stripping). In some cases, additional stripping caused the detachment of the entire titanium layer from its substrate, and in other cases, contamination of the resulting surface, presumably with the adhesive from the tape, was readily detected by XPS (not shown).

In contrast, samples prepared by evaporating titanium on mica coated with a sufficiently thick layer of carbon (between 6 and 20 nm) were found to be completely free from mica residue after stripping (Figure 2c,d).

The ability of the XPS technique to provide information concerning the oxidation state of the elements detected on the surface was exploited for determining the nature of the exposed titanium species (Figure 3). On the Zürich samples prepared without the use of a carbon layer and that were not treated with plasma prior to XPS analysis, the Ti 2p peaks were found to consist of two superimposed doublets, corresponding to a mixture of titanium oxide and metallic titanium. The difference in binding energy between the Ti 2p_{3/2} signals of TiO₂ and of metallic titanium was found to be 5 eV, in good agreement with the literature value (Figure 3a).²⁰

On the samples that were plasma-cleaned, the Ti 2p peak appeared as a single, well-defined, spin-split doublet, with the typical interval of about 6 eV between its two peaks (i.e., Ti 2p_{1/2} and Ti 2p_{3/2}, Figure 3b). The binding energies of the peaks within the doublet were found to be 464.8 ± 0.5 eV for the Ti 2p_{1/2} signal and 459.0 ± 0.4 eV for the Ti 2p_{3/2} signal, also in good agreement with the binding energies of TiO₂ found in the literature (464.34 eV for the

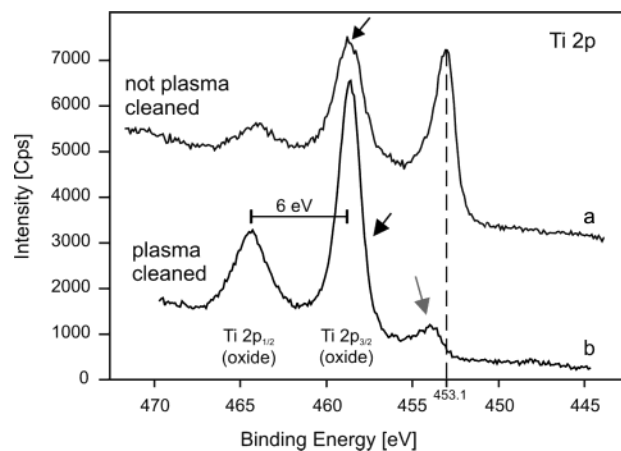


Figure 3. Influence of the plasma cleaning on the surface composition of the template-stripped samples. Mica residue was detected on both samples. (a) Detailed spectrum of the Ti 2p peak acquired on a sample prepared by the conventional template-stripping method (sample Z-8). Most of the titanium present is in one of the two oxidation states corresponding to metallic titanium (Ti 2p_{3/2} peak at 453.1 eV) and TiO₂ (Ti 2p_{3/2} peak at 458.1 eV). The difference of 5 eV between the binding energies of these two species is consistent with the values found in the literature.²⁰ The peak in the middle (arrow) results from a superposition of the 2p_{1/2} peak of the metallic titanium (experimentally found values 458.9–459.1 eV) and the 2p_{3/2} peak of TiO₂ (experimentally found values 458.3–458.5 eV). (b) Same as in (a), but on a sample exposed to oxygen plasma for 3 min (sample Z-7). Most of the titanium is present as TiO₂ (Ti 2p doublet at 458.6 and 464.4 eV). The energy difference between the middle peak (black arrow) and the smaller one (gray arrow) at 454.0 eV is less than 5 eV, suggesting that the latter peak arises from lower oxides rather than from metallic titanium. The bar highlights the 6 eV interval between the two signals of the spin-split Ti 2p doublet.

Ti 2p_{1/2} peak and 458.8 eV for the Ti 2p_{3/2} peak²¹). Therefore, most of the titanium present at the exposed interface was oxidized during plasma treatment. This is consistent with what is expected of a highly reactive metal such as titanium, which is known to build a thin (3–4 nm thick) oxide layer within seconds upon exposure to air.¹¹ Treatments such as anodization or oxygen plasma result in the formation of films much thicker than the information depth of XPS,²² which for titanium oxide (TiO₂) is approximately 7–8 nm for the experimental XPS conditions used in this work.²⁰

In addition to the doublet arising from TiO₂, a smaller peak was observed at 454.0 eV (see the arrow on curve b in Figure 3). It is less than 5 eV away from the Ti 2p_{3/2} signal of the oxide doublet, and does not correspond to metallic titanium, but rather to lower oxides (TiO_x, x < 2). It can therefore be concluded that, after plasma cleaning, metallic titanium is absent from the top ~10 nm of the surface, and that the oxide–metal interface contains lower oxide species. This is consistent with the observation of TiO and Ti₂O₃ species at the interface between metal and native oxide film.²⁰ The observations made on the plasma-cleaned Bristol samples which lacked titanium carbide (see below) were consistent with the above picture.

(21) Moulder, J. F.; Stickle, W. F.; Sobol, P. E.; Bomben, K. D. *Handbook of X-ray photoelectron spectroscopy*; Physical Electronics Division, Perkin-Elmer Corp.: Eden Prairie, MN, 1992.

(22) Lausmaa, J. Mechanical, Thermal, Chemical and Electrochemical Surface Treatment of Titanium. In *Titanium in Medicine: Material Science, Surface Science, Engineering, Biological Responses and Medical Applications*; Thomsen, P., Ed.; Springer-Verlag: Heidelberg and Berlin, 2001; pp 231–266.

(20) Sittig, C. E. Charakterisierung der Oxidschichten auf Titan und Titanlegierungen sowie deren Reaktionen in Kontakt mit biologisch relevanten Modellösungen. Dissertation Nr. 12657, ETH Zürich, 1998.

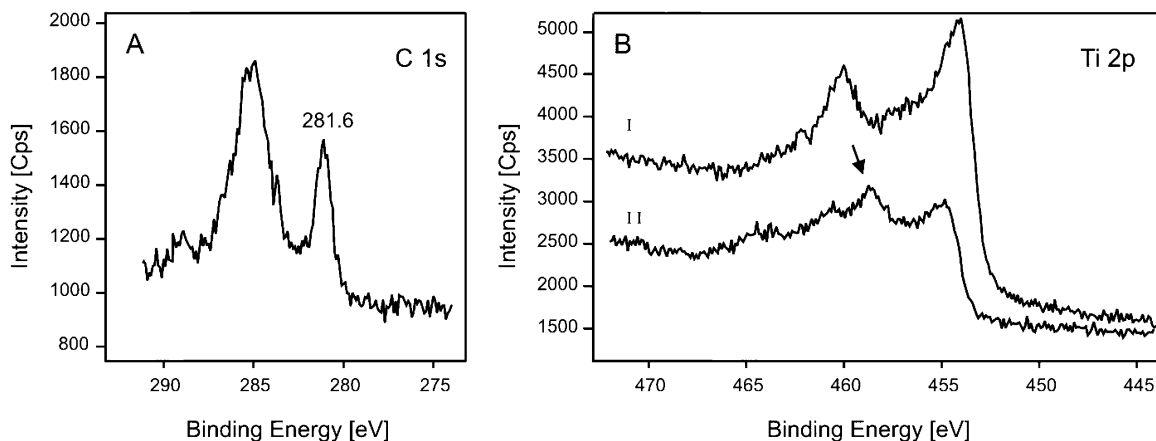


Figure 4. XPS analysis of samples containing titanium carbide (samples B-3 and B-6). (a) Detailed spectrum of the C 1s region. The peak at 285.0 eV results from hydrocarbon contamination, and the one at 281.6 eV from TiC. (b) Detailed spectrum of the Ti 2p peak with a doublet corresponding to a low oxidation state of titanium (curve I, sample not plasma cleaned). The contribution of titanium oxide to the overall signal becomes slightly more pronounced after plasma cleaning (curve II, arrow pointing to the peak at 458.8 eV).

The analysis of the high-resolution XPS spectra of the carbon 1s peaks (Figure 4a) on about half of the Bristol samples led to the surprising discovery of titanium carbide on their surface (see the peak at 281.6 eV in Figure 4a).²¹ On the Zürich samples (even those prepared on the carbon-coated mica) this peak has never been observed. The presence of titanium carbide species markedly influences the appearance of the Ti 2p peak, because it causes the presence of another doublet superimposed onto those arising from the metallic titanium and the various titanium oxides.²³ This effect explains the shape of the titanium peaks observed on these samples (Figure 4b). Oxygen plasma treatment had only limited influence on the structure of the Ti peaks on these samples (cf. Figures 3b and 4b).

Angle-Resolved XPS and Depth Profiling. The surface composition of two of the Bristol samples as a function of depth was analyzed by angle-resolved XPS (Figure 5a–d), and by argon ion depth profiling (Figure 5e,f).

In Figure 5a, the atomic percentage for each element is plotted as a function of takeoff angle (i.e., the sampling depth). It is clear that the signal arising from hydrocarbon contamination decreases, while that arising from titanium increases with the sampling depth. The signals due to K, Al, and Si—elements comprising mica—remain more-or-less constant, while that due to titanium carbide increases slightly. Detailed spectra of the titanium 2p peak shown in Figure 5b clearly show that the topmost portion of the surface is essentially devoid of titanium (curve at $\alpha = 15^\circ$ in Figure 5b). The most superficial titanium appears to be partially oxidized (Figure 5c).

The same trends (results not shown) were found for angle-resolved XPS measurements performed on an instrument with a much smaller detection area (0.16 mm², as opposed to 28.3 mm² that was used in the measurements described above).

The results of depth profiling (Figure 5e,f) compare well with those of the angle-resolved XPS discussed above. In particular, the signal due to Ti is seen to increase markedly as more of the superficial material is sputtered away. The total intensity of the C 1s peak (that is the sum of the contributions from the hydrocarbon contamination and from titanium carbide) increases slightly with sputtering

time (Figure 5f), while its energy shifts from 285.0 eV—the value typical of hydrocarbon contamination—to about 282.0 eV, approaching the value corresponding to that of titanium carbide (281.6 eV, result not shown). The O 1s peak also displays, in addition to a significant decrease in intensity (Figure 5f), a shift toward smaller binding energies (result not shown). The binding energies of the O 1s in titanium oxides (TiO₂, Ti₂O₃, and TiO) have smaller values than in Al₂O₃ and SiO₂ (529.9–530.8 eV for the former and approximately 531 and 533 eV for the latter).^{21,24,25} Therefore, this shift in the oxygen signal is caused by the chemical nature of the oxygen changing, as a function of depth, from the oxides comprising the mica to the titanium oxides.

An important difference between the results obtained with the two techniques (angle-resolved XPS and depth profiling) is apparent when the behavior of the elements comprising mica are compared. In the case of angle-resolved XPS (Figure 5a), the relative atomic percentages of Si, Al, and K remain constant as a function of takeoff angle (penetration depth), while they are observed to decrease rapidly when the sample is examined by depth profiling (Figure 5e). This effect can be understood if the layered nature of the interface is considered. In the case of depth profiling, the material is being physically removed and no longer contributes to the spectra collected from the deeper regions of the interface. Hence, the results of the depth profiling (Figure 5e,f) leave no doubt as far as the relative locations of mica and titanium (since mica is removed first, it is located above). In the case of angle-resolved spectra, on the other hand, the sampling depth changes with the angle. While with increasing emission angle the relative contribution of the uppermost portions of the interface decreases, and that due to the contribution from the lower layers increases, the contribution from an intermediate layer will appear more-or-less constant. In this case, the topmost layers of the sample include the carbon species (due to hydrocarbon contamination or the carbon normally present between the mica planes; see the Discussion), while the bottommost (in terms of the sampling depth) include the titanium species. Mica is located in between. Similar effects have been described

(23) Ihara, H.; Kumashiro, Y.; Itoh, A.; Maeda, K. *Jpn. J. Appl. Phys.* **1973**, *12*, 1462–1463.

(24) Ramqvist, L.; Hamrin, K.; Johansson, G.; Fahlman, A.; Nordling, C. *J. Phys. Chem. Solids* **1969**, *30*, 1835–1847.

(25) Werfel, F.; Brummer, O. *Phys. Scr.* **1983**, *28*, 92–96.

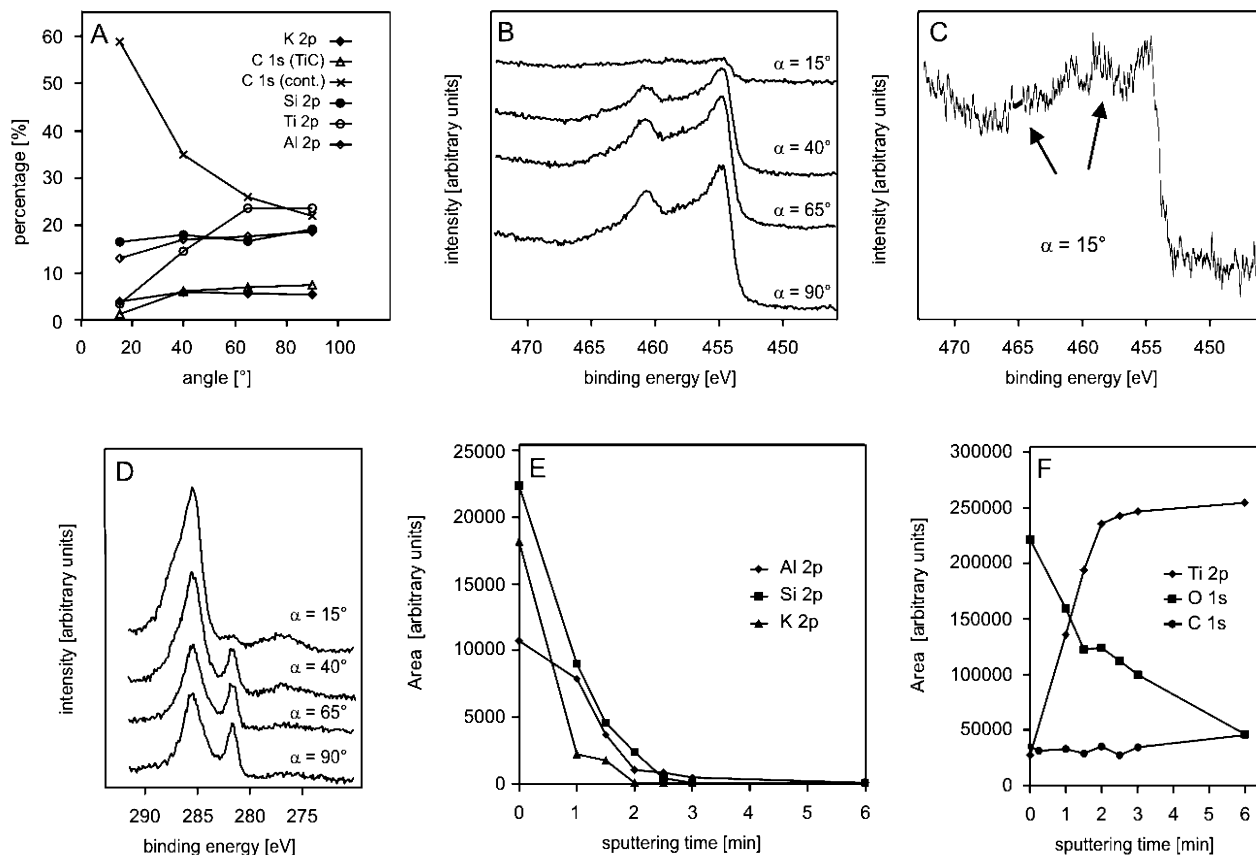


Figure 5. Elemental composition of the surface investigated by angle-resolved XPS and depth profiling. (a) Percentages of the elements that were detected plotted as a function of electron takeoff angle. The hydrocarbon and titanium carbide contributions to the C 1s peak are given as separate curves. The former decreases with increasing detection depth, while the latter increases; their sum slightly increases with detection depth. (b) Detailed spectra of the Ti 2p peak recorded at various takeoff angles. The peak's intensity is seen to increase markedly with the sampling depth (i.e., with increasing angle), indicating that only a small amount of titanium is present at the very top of the surface (curve at $\alpha = 15^\circ$). The binding energies of the peaks within the doublet are 454.8 eV (Ti 2p_{3/2}) and 460.7 eV (Ti 2p_{1/2}) and correspond to titanium carbide and/or a lower oxide of titanium. (c) Detailed spectrum of the Ti 2p peak recorded at a grazing angle of 15°. Two doublets are recognizable: one at binding energies of 454.8 eV (2p_{3/2}) and 460.7 eV (2p_{1/2}), and the other at 458.6 eV (2p_{3/2}) and 464.1 eV (2p_{1/2}) (pointed to with arrows). The latter corresponds to titanium oxide. (d) Detailed spectra of the C 1s region recorded at various takeoff angles. The signal due to hydrocarbon contamination (at 285.0 eV) diminishes with increasing detection depth, while the TiC signal (281.6 eV) increases. (e) Areas of the Al, Si, and K peaks as a function of sputtering time. (f) Areas of the Ti, O, and C peaks as a function of sputtering time. A clear increase in the area of the titanium peak is apparent, while all the other elements except carbon progressively disappear with increasing depth.

in the literature, e.g., for alkyl phosphate self-assembled monolayers on tantalum pentoxide.²⁶

X-ray Photoelectron Diffraction. Photoelectrons emitted from a well-ordered single-crystalline surface exhibit strong-intensity modulations as a function of emission direction. The modulations are due to photoelectron scattering and wave interference within the sample and can be investigated to obtain information about the lattice structure of a surface by means of XPD.¹⁸ XPD plots of the Al 2p peak collected on a Bristol titanium sample and of freshly cleaved mica are shown in Figure 6. Although the diffraction spots recorded on the titanium sample (Figure 6a) are rather poorly defined, the symmetry of the ordered structure that is detected is still recognizable and corresponds to that of mica (Figure 6b). The poor definition of the diffraction spots in Figure 6a suggests that only a few planes (approximately half of a unit cell of mica²⁷) contribute to the diffraction pattern, indicating that there is a very thin mica layer on top of the titanium (thick islands of small lateral dimensions would yield more

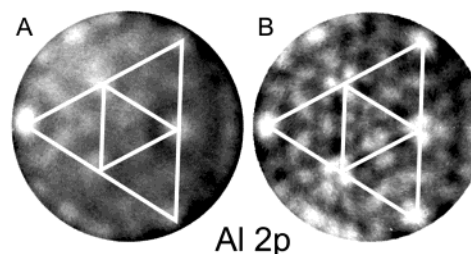


Figure 6. XPD plots acquired at 74.3 eV (Al 2p peak) on a sample prepared by the template-stripping method (sample B-7, panel a) and on mica (b; mica was cleaved as described in ref 37). The similarity in the structures resolved by XPD on the two samples is quite apparent. The 3-fold symmetry of the diffraction spots, which arises due to the arrangement of the Al atoms between the oxygen octahedra,³⁸ is outlined with white triangles. The diffraction spots in (a) are poorly defined, suggesting that only a few planes contribute to the diffraction pattern.

defined spots instead^{28,29}). The XPD plots of the Si 2p, Ti 2p, and C 1s peaks were recorded as well (results not

(26) Textor, M.; Ruiz, L.; Hofer, R.; Rossi, A.; Feldman, K.; Hähner, G.; Spencer, N. D. *Langmuir* **2000**, *16*, 3257–3271.

(27) Gröning, P. University of Fribourg, Switzerland. Personal communication.

(28) Omori, S.; Ishii, H.; Nihei, Y. *J. Electron Spectrosc. Relat. Phenom.* **1998**, *88–91*, 517–522.

(29) Schwaller, P.; Gröning, P. University of Fribourg, Switzerland. Personal communication.

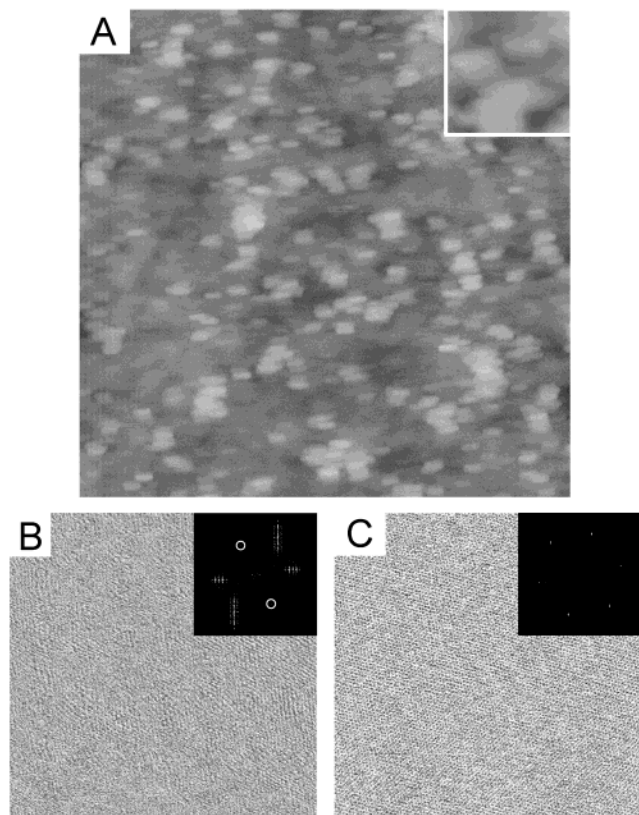


Figure 7. Surface structure of a sample prepared by the template-stripping method investigated by AFM. (a) Overview of the surface of sample B-6 (the sample was not plasma cleaned). Oxide domes, with dimensions of about 50×100 nm, are visible. Scan size: $2.5 \mu\text{m}$. Z -range: 5 nm. Inset scan size: 250 nm. Inset z range: 2.5 nm. (b) High-resolution image recorded on top of one of the domes shown in (a). The inset shows the Fourier transform of the image. The white circles highlight the weak spots present in their center. Scan size: 40 nm. Z -range: 2 nm. (c) High-resolution image of mica. The Fourier transform is shown in the inset. Scan size: 50 nm. Z -range: 0.6 nm.

shown), and only in the case of Si could an ordered structure be found (the symmetry of which, once again, corresponded to that of mica).

Atomic Force Microscopy. Upon investigation of the template-stripped titanium samples by means of AFM (Figure 7, Bristol sample), it was found that the surface of the samples was rather wavy and exhibited dome-shaped features that were attributed to growing titanium oxide islands. These “domes” were very numerous and small when the surface had undergone a plasma cleaning (not shown), while they were larger and fewer in number if the surface was merely exposed to air. Oxide domes form on the surface of metallic titanium because the unit cell of the oxide is larger than that of the metal, resulting in high compressive stresses.^{30,31} The dependence of size and number of the domes on the atmosphere the samples were exposed to (air vs oxygen plasma) can be explained in terms of the number of oxidation nucleation points in the two cases: in a plasma treatment the nucleation points will be more numerous than when the sample is exposed to air.

The high-resolution images obtained on the surface of a template-stripped titanium sample and on that of freshly cleaved mica are compared in Figure 7b,c. The insets in

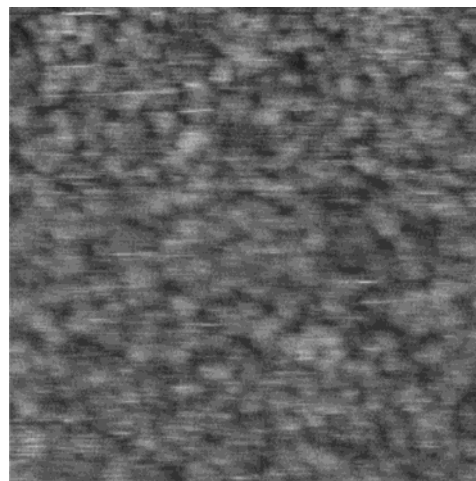


Figure 8. Representative AFM image of a sample prepared by evaporating a titanium oxide onto mica coated with a 14 nm carbon layer. The surface is not atomically flat, and grains of an average size of about 15 nm are clearly visible. This sample was prepared without annealing the mica at 300°C before and after the deposition of titanium, as a part of an investigation into the effect of the annealing temperature on the size of the grains. Scan size: 300 nm. z range: 5 nm.

these panels are the Fourier transforms of the respective AFM images. In the case of mica, the familiar hexagonal pattern is visible in the image and six evenly spaced spots ($R = 0.524 \pm 0.009$ nm) are visible on the Fourier transform. The images acquired on the titanium samples were always worse in terms of quality. This was reflected in the quality of their Fourier transforms—by the appearance of the split peaks (Figure 7c), satellites, and other artifacts. However, most of the images resulted in Fourier transforms corresponding to a (distorted) hexagonal lattice, and none corresponded to any of the possible structures formed by titanium oxide³² or metal.³³ The distortion can be explained by the fact that on top of the titanium oxide domes the mica surface is bent and its structure deformed.

Titanium oxide domes were also observed on the samples prepared by evaporating the oxide onto carbon-coated mica (Figure 8).

Discussion

The presence of mica on the surface of the samples prepared by the template-stripping method (Figure 2) raises some concern with respect to the usefulness of this method for obtaining model, flat titanium oxide surfaces for protein-adsorption studies. The combination of techniques used in this study for investigating the titanium–mica interface allows a fairly consistent picture of its organization to be painted. On one hand, there is the possibility that the remnants of mica are present as isolated islands, with the titanium oxide surface exposed in between. On the other hand, there is the possibility that a confluent, very thin—few unit cells—layer of mica is present on the surface, and very little, if any, titanium oxide is exposed. However attractive the first scenario might seem, it is not consistent with the experimental observations presented above. It has already been mentioned in the Results that the angle-resolved XPS and

(32) *CRC Handbook of Chemistry and Physics*, 75th ed.; Lide, D. R., Frederikse, H. P. R., Eds.; CRC Press: Boca Raton, FL, 1994.

(33) *Materials properties handbook: titanium alloys*; Boyer, R., Welsch, G., Collings, E. W., Eds.; ASM International: Materials Park, OH, 1994.

(30) Brown, G. M. *J. Vac. Sci. Technol., A* **1992**, *10*, 3001–3006.

(31) Bawinger, J. P.; Orme, C. A.; Gilbert, J. L. *Surf. Sci.* **2001**, *491*, 370–387.

depth-profiling (Figure 5) data can be successfully interpreted in terms of a layered model (hydrocarbon contamination–mica–titanium species). Furthermore, in the case where both of the materials (mica and titanium oxide; one would expect them to be covered with a layer of hydrocarbon contamination to similar degrees) have zones at the very top of the surface, the signals arising from both species would have an almost constant intensity at all detection angles. Also consistent with this interpretation (thin, confluent layer of mica) are the results of XPD (Figure 6) and of AFM (Figure 7).

The observation of a mica-like structure on top of the titanium oxide domes with AFM (Figure 7) is striking in itself, for it suggests that the binding between the two materials is strong enough to withstand the stress of the oxide domes growing underneath the mica on one hand, and that the metal is capable of reacting underneath the mica on the other. XPS results also suggested that, despite the presence of mica, titanium oxide was present in the samples subjected to oxygen plasma treatment (Bristol samples which did not contain titanium carbide (results not shown), and the plasma-cleaned Zürich samples, Figure 3). This may suggest that the “nonstripped” titanium–mica sandwiches are also prone to oxidation and will age if stored in air. The observation that cleaving of the samples was found to be increasingly more difficult as their age increased³⁴ lends some support to the aging hypothesis.

The presence of titanium carbide in the Bristol samples, as well as the apparent contradiction between the results of this study and those of Cacciafesta et al.¹² (20% of all samples analyzed with XPS by Cacciafesta et al.¹² were found not to contain mica residue³⁵), prompted a more detailed investigation into how carbon, normally present between the mica layers,²⁷ may affect the properties of the titanium–mica sandwiches. For this purpose carbon-coated mica was used in the sample preparation (Figure 1), and indeed, a mica-free titanium oxide surface was obtained (Figure 2). On most of the samples, the presence of large amounts of carbon on the sample surface after cleavage necessitated the use of oxygen plasma treatment to observe the underlying titanium. In our hands, the resulting surfaces were never flat but exhibited a grainy structure (Figure 8). The size of the grains was found to depend on the carbon thickness (varied between ~6 and ~20 nm) and temperature at which the evaporation of titanium was performed (varied between 25 and 300 °C); however, quantitative investigation of these dependencies was not undertaken. It should be kept in mind that the properties of the amorphous carbon obtained by evaporation may be quite different from those of the carbon naturally present in the micas; in the latter case, very thin graphite films have been identified for certain mica samples by XPD.²⁷ Support for this assertion comes from the observation that, despite the abundance of carbon, no titanium carbide was detected in any of the samples prepared with the carbon-coated mica. It is also rather unlikely that even 6 nm of carbon could be present between the cleavage planes of a naturally occurring mineral with a plane–plane spacing of ~1 nm.³⁶

(34) Cacciafesta, P. University of Bristol, U.K. Personal communication.

(35) Cacciafesta, P.; Jandt, K. D. University of Bristol, U.K. Personal communication.

Conclusions

This study focused on the characterization of the titanium (oxide) surfaces prepared by evaporating titanium onto a freshly cleaved surface of resistively heated mica (following the so-called template-stripping method¹³ as described in Cacciafesta et al.¹²). Both samples prepared by Cacciafesta et al.¹² and those prepared in-house using an identical procedure were investigated, and were found to contain a thin (few unit cells), nearly confluent layer of mica that could not be removed by stripping. Underneath the mica, the titanium species (titanium oxide and, on some samples, titanium carbide) were found to be disordered, while ordering consistent with that of mica was clearly detected by both atomic force microscopy and X-ray photoelectron diffraction. The appearance of the oxide underneath the mica suggested that aging of the samples has taken place. These results are in contradiction with those reported by Cacciafesta et al.¹²

If a layer of amorphous carbon was introduced between the mica and the titanium, no mica could be detected on the surface after the stripping step, and a clean titanium oxide surface was recovered after the carbon layer was removed by oxygen plasma cleaning. Possibly, the carbon naturally present in the micas can play a role similar to that of the artificially introduced one and may be one of the potential reasons for the discrepancies between the results of Cacciafesta et al.¹² and ours.

None of the samples, whether prepared by the conventional template-stripping protocol or a modified one (using carbon-coated mica), exhibited flat surfaces, but presented well-defined titanium oxide domes on their surface.

Acknowledgment. We thank Dr. Paola Cacciafesta and Prof. Klaus D. Jandt (formerly at the University of Bristol, Bristol, U.K.) for supplying their samples for analysis and for constructive discussion, Dr. Davide Ferri and Prof. Alfons Baiker (Chemistry Department, ETH Zürich) for allowing F.F.R. and I.R. to use their evaporator facilities, Dr. Kirill Feldman and Dr. Christian Dicke (Department of Materials, ETH Zürich) for introducing them to its operation for preparing ultraflat gold samples, Dr. Martin Müller (Department of Biology, ETH-Zürich) for allowing them to use the evaporator facility for preparing carbon-coated mica, Ms. Irene Klingenfuss, Dr. Samuele Tosatti, Dr. Roger Michel, and Dr. Vinz Frauchiger (Department of Materials, ETH Zürich) for help with the XPS and with the analysis of the XPS data, Dr. Patrick Schwaller, Dr. Pierangelo Gröning, and Prof. Louis Schlapbach (Solid State Physics Group, University of Fribourg, Switzerland) for allowing F.F.R. to use their XPD instrument and for help with the analysis of the XPD data, Dr. Jane Beringer (Lawrence Livermore National Laboratory, Livermore, CA) for insightful suggestions, and Prof. Nicholas D. Spencer (Department of Materials, ETH Zürich) for critical comments about this manuscript. The TOP NANO 21 Research Program of the ETH Council is gratefully acknowledged for funding.

LA034280I

(36) Bailey, S. W. *Rev. Mineral.* **1984**, *13*, 1–60. Cited in Muller, D. J.; Amrein, M.; Engel, A. *J. Struct. Biol.* **1997**, *119*, 172–188.

(37) Carpick, R. W.; Agrait, N.; Ogletree, D. F.; Salmeron, M. *J. Vac. Sci. Technol., B* **1996**, *14*, 1289–1295.

(38) Kuwahara, Y. *Phys. Chem. Miner.* **1999**, *26*, 198–205.